Proc. Natl. Acad. Sci. USA
Vol. 77, No. 1, pp. 343–346, January 1980
Biophysics

Electron spin resonance of ^{17}O-labeled protein–peroxide radicals: Zein and edestin

(oxygenated free radicals/electron spin resonance spectra/^{17}O hyperfine structure)

LOUIS J. DIMMEY* AND WALTER GORDY

Department of Physics, Duke University, Durham, North Carolina 27706

Contributed by Walter Gordy, October 22, 1979

ABSTRACT **Hyperfine structure due to ^{17}O has been measured in irradiated zein and edestin after exposure to gaseous oxygen with ^{17}O concentrated to 24%. The observations prove that the free radicals produced by ionizing irradiation under vacuum at 300 K are converted by the oxygen to protein–peroxide free radicals $X—O^{(1)}—O^{(2)}$, with the unpaired electron density in a π-type orbital predominantly on the peroxide group. From the observed couplings, the $2p_\pi$ spin densities on zein–peroxide are found to be 0.29 and 0.45 for $O^{(1)}$ and $O^{(2)}$, respectively; those on edestin–peroxide are 0.26 and 0.48 for $O^{(1)}$ and $O^{(2)}$, respectively.**

In the first observations of electron spin resonance (ESR) signals in irradiated proteins (1), a proton hyperfine doublet produced from bone collagen was found to be converted to a singlet when the specimen irradiated in vacuum was exposed to oxygen. It was postulated that that O_2 combined with the free radicals in the irradiated sample to produce a protein–peroxide free radical. Since this initial finding, many examples of this oxygen effect have been observed for other proteins (2) as well as for biochemicals of other types (3). In certain proteins such as zein and edestin, chosen for the present ^{17}O study, the conversion of the proton multiplet to the oxygen singlet is rapid, with complete conversion to the singlet occurring within minutes after exposure of the sample to atmospheric oxygen. In others, most notably silk, the oxygen effect is slow, requiring days of exposure for partial conversion. This slower conversion is believed to result from steric factors that hinder or prevent the molecules of oxygen from reaching the free-radical centers in fibrous proteins such as silk. The oxygen effect is not observed for sulfur-centered radicals produced by irradiation of proteins, probably because molecular oxygen does not combine with the sulfide free radicals.

The earlier studies of the oxygen effect in irradiated proteins were made with ^{16}O, which has no hyperfine structure. Although there seems to be little doubt that the radicals formed upon admission of oxygen are peroxide radicals, the present study of ^{17}O-labeled radicals unquestionably confirms this interpretation and, in addition, provides new information about the electronic structure of the protein–peroxide radicals.

In many irradiated proteins, including edestin and zein, the free-radical site giving the ESR pattern in the absence of oxygen is believed to be the C_α—R group in structure **I**

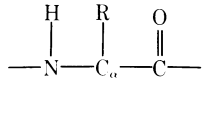

I

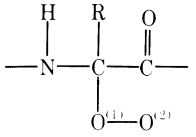

II

formed by loss of a H from a carbon of the polypeptide chain. For edestin under vacuum, a proton doublet like that for the $C_\alpha H$ fragment in irradiated polyglycine is formed (2), which indicates that R = H and that the radical is formed in the glycine unit. A similar doublet is observed for evacuated zein, but with a superimposed quartet like that for polyalanine (2). This indicates formation of radical sites in both glycine and alanine ($R = CH_3$) units of zein. Relative intensities of the superimposed patterns indicate that formation in the alanine unit is somewhat less than that in the glycine unit. Both patterns are converted to singlets when normal oxygen ($^{16}O_2$) is admitted to the irradiated sample.

Upon exposure of the irradiated samples to oxygen, peroxide radical **II** is evidently formed. When this occurs, as the present study confirms, the spin density of **I** is effectively transferred to the captured O_2, where its interaction with the protons of the R group is insufficient to produce a resolvable proton splitting. Although ^{16}O has no hyperfine structure, the substituted ^{17}O has nuclear spin $I = 5/2$, which gives rise to a sextet ESR splitting by each of the inequivalent oxygens in peroxide radical **II**.

Previously, ^{17}O hyperfine structure has been observed for randomly oriented peroxide radicals of irradiated polytetrafluoroethylene (4) and for oriented peroxide radicals $C_{10}H_{11}OO$ in single crystals (5). Also, the isotropic component of the ^{17}O hyperfine structure has been observed for some simpler peroxide free radicals in liquid solutions (6, 7). These earlier observations have been helpful to us in our analysis of the ^{17}O hyperfine structure for the protein–peroxide radicals.

EXPERIMENTAL PROCEDURES

A balanced-bridge, X-band ESR spectrometer operated at a frequency of 9000 MHz was used for these measurements. Evacuated tubes made of Spectrosil quartz held the protein powders, which were placed in a ^{60}Co γ-ray source for irradiation at 300 K. Doses were approximately 3×10^5 rads (300 grays). Afterward, the tubes were annealed in a gas/oxygen flame to eliminate any free radicals formed in the quartz.

Exposure of the irradiated samples to normal gaseous oxygen or to ^{17}O concentrated gas was accomplished in this way. The tube was connected to a flask of the oxygen gas, the glassware between them was evacuated, and the flask was immersed in liquid nitrogen. When the valve on the flask was opened, the oxygen at its vapor pressure at 77 K (about 130 torr) flowed into the sample tube. After the sample was disconnected from the flask, it was ready for observation in the spectrometer. Conversion of the radicals formed under vacuum to peroxides required 2–4 hr. The enriched oxygen gas contained 24% ^{17}O atoms.

Abbreviation: ESR, electron spin resonance.

* Present address: School of Engineering, Duke University, Durham, NC 27706.

OBSERVED SPECTRA

Fig. 1 shows a comparison of the second-derivative spectra of irradiated zein after exposure to normal oxygen gas and after similar exposure to gas with 24% substitution of ^{17}O atoms for ^{16}O atoms. The spectrometer amplification for the two curves was approximately the same. The stick diagrams at the base correspond to the theoretically expected ^{17}O hyperfine patterns of the two forms, X—^{16}O—^{17}O and X—^{17}O—^{16}O. Hyperfine components for the less-probable species, X—^{17}O—^{17}O, proved to be too weak for detection. The pattern with the wider span is that for X—^{16}O—^{17}O. Fig. 2 shows the curve obtained for irradiated edestin after exposure to the ^{17}O-substituted gas.

The nature of the ESR signals and of the free radicals formed upon irradiation in the absence of oxygen are described in the Introduction. For both proteins, the primary radicals are believed to have the general structure **I** and the peroxide radicals (secondary) to have structure **II**. The hyperfine structure and g values for these protein–peroxide radicals are explained in the following paragraphs.

HYPERFINE STRUCTURE

The analysis of ESR hyperfine structure for randomly oriented free radicals is now well known (ref. 8, pp. 353–441). The shapes of the observed absorption curves depend on several factors, the most important of which are the anisotropy in the **g** tensor and in the nuclear coupling tensors. In the protein–peroxide

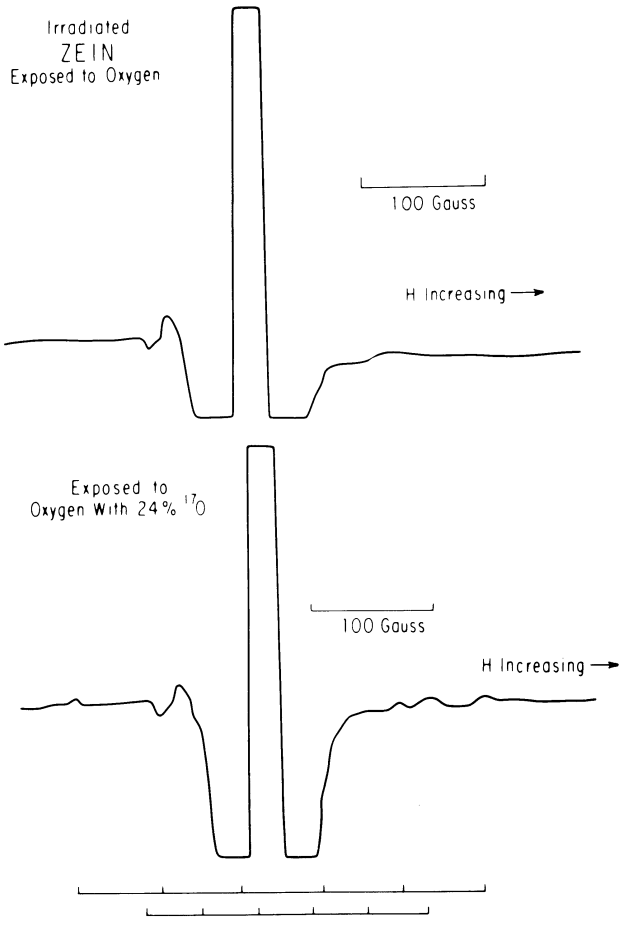

FIG. 1. Second-derivative ESR spectrum of γ-irradiated zein after exposure to gaseous $^{16}O_2$ (*Upper*) and after exposure to oxygen gas enriched with 24% ^{17}O (*Lower*).

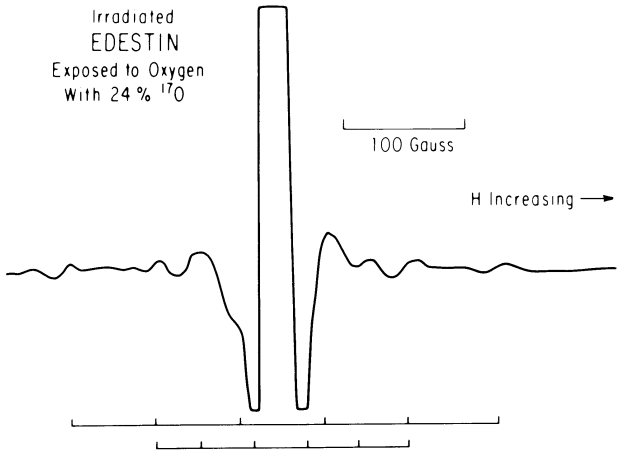

FIG. 2. Second-derivative ESR spectrum of γ-irradiated edestin after exposure to oxygen gas enriched with 24% ^{17}O.

radicals considered here, the isotropic component A_f of the ^{17}O coupling is of comparable magnitude to the anisotropic coupling B and is of like sign. Consequently, the resultant coupling $(A_f - B)$ for the magnetic field of orientations perpendicular to the p_π orbital of the unpaired electron is very small. As a result, the critical absorptions corresponding to the perpendicular-field orientation are not resolvable and are not separable from the strong ^{16}O singlet absorption. To obtain a value for B, one must observe the much weaker critical absorptions corresponding to orientation of the field approximately parallel to the coupling p_π orbital of the ^{17}O atoms.

The nature of the ^{17}O hyperfine spectra is illustrated by the idealized curves of Fig. 3, in which line-broadening factors are neglected except those of the anisotropy in the nuclear coupling and in **g**. Also, for simplification of the diagram, **g** as well as **A** is assumed to be axially symmetric about the directions of the coupling p_π orbital. The weak peaks in the observed derivative curves (Figs. 1 and 2) correspond to the outer terminations of the different ^{17}O component absorptions. If the coupling constant is expressed in magnetic-field units, these outer peaks occur at the critical field values,

$$H_\parallel = h\nu_0/(g_\parallel\beta) + A_\parallel M_I, \qquad [1]$$

where ν_0 is the operating frequency and $g_\parallel = g_u$ is the effective g value for **H** along the coupling p_π orbital, and

$$A_\parallel = A_f + 2B, \qquad [2]$$

where $A_\parallel$ is the effective coupling constant for **H** along the coupling p_π orbital. The much stronger unresolvable inside-component terminations occur at

$$H_\perp = h\nu_0/(g_\perp\beta) + A_\perp M_I, \qquad [3]$$

where $g_\perp$ is the effective g value for **H** imposed in the plane perpendicular to the p_π orbital, and

$$A_\perp = A_f - B. \qquad [4]$$

Although $g_\parallel$ has a fixed value, $g_\perp$ ranges in value from g_v *to* g_w. However, for simplicity in Fig. 3, g_v was chosen as the particular value for $g_\perp$. The quantum numbers are $M_I = \pm 5/2$, $\pm 3/2$, $\pm 1/2$, corresponding to the spin $I = 5/2$ for ^{17}O. The coupling constants have the same sign and are both negative because the nuclear magnetic moment of ^{17}O is negative.

The fact that the $H_\perp$ components cannot be resolved or separated from the unsubstituted ^{16}O absorption indicates that $A_f \approx B$. With $A_f = B$, the observed component separation of

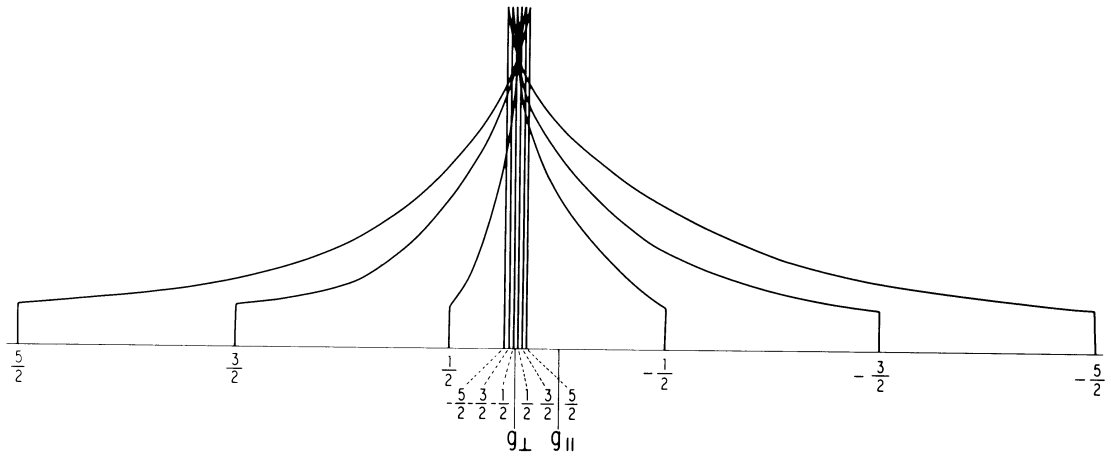

FIG. 3. Idealized theoretical pattern of ESR hyperfine structure for a coupling ^{17}O of randomly oriented peroxide radicals having axial symmetry in coupling with $A_\perp = A_f - B = 2.5$ G and with $A_\parallel = -71$ G, as for $^{17}O^{(2)}$ of edestin peroxide. For simplicity, the **g** tensor is also assumed to have axial symmetry about the coupling $2p$ orbital with $g_\parallel = g_u$ and $g_\perp = g_v$ for edestin. Line-broadening factors other than anisotropies in **g** and **A** are neglected.

71 G for $^{17}O^{(2)}$ in edestin-peroxide gives with Eq. **2** the value $A_f = B = 23.7$ G for the terminal oxygen; and the observed component separation of 42 G for $^{17}O^{(1)}$ gives $A_f = B = 14$ G for the central oxygen. However, we believe that more accurate values for B are obtained with the assumption that $A_f(^{17}O^{(1)}) = 16$ G and $A_f(^{17}O^{(2)}) = 22$ G, as measured for the radicals $(CH_3)_2$ COO and $C_6H_5(CH_3)_2COO$ in liquid solution (7). These values are close to the isotropic coupling observed in diverse peroxide radicals (5–7) in which the O_2 is bonded to a carbon. With these values assumed for A_f in both zein and edestin, the anisotropic coupling constants calculated with Eq. **2** are as listed in Table 1. The couplings $A_\parallel$ in MHz are related to the component separations in gauss by

$$A_\parallel(\text{MHz}) = 1.40 g_\parallel \Delta H(\text{G}). \quad [5]$$

PRINCIPAL g VALUES

The principal g values of these protein-peroxide radicals cannot be accurately derived from the randomly oriented radicals, but approximated values have been deduced by the following procedure. The weak peak to the left of the strong central absorption in the unsubstituted ^{16}O peroxides, shown for zein in Fig. 1 *Upper*, evidently corresponds to the maximum g value, g_w. The value determined by this peak is $g_w = 2.044$ for the zein peroxide. The value similarly obtained for the edestin is 2.040. These values are in the range of those derived for the peroxide radical in single-crystal measurements (ref. 8, p. 602). For example, in the $C_{10}H_{11}OO$ radical, $g_w = 2.045$ and 2.039 for the two crystal sites (5). The g_w values are expected from theory to be directed approximately along the O—O bond axis. Peaks corresponding to the intermediate and minimum g values, g_v and g_u, respectively, cannot be separated for the unsubstituted ^{16}O radicals; both of them are evidently within the strong central absorption with the center corresponding to 2.007 for zein and to 2.006 for edestin. However, the minimum value g_u is expected from theory to have the direction of the p_π orbital, that for which the ^{17}O hyperfine components are measured. Thus, if slight second-order shifts are neglected, the g_u value corresponds to the center of the $A_\parallel M_I$ hyperfine pattern like that shown in Fig. 3. We have assumed that the intermediate values g_v correspond to those for the strong central absorption for the unsubstituted ^{16}O radicals. The unresolved $A_\perp M_I$ pattern is depicted as a closely spaced multiplet centered near g_v in Fig. 3. This multiplet evidently falls under the strong central $^{16}O_2$ absorption. For orientations of the magnetic field along or near g_w, the ^{17}O components are too weak for observation. The approximate g values derived by these procedures and assumptions are listed in Table 2. They are close to the values 2.0026, 2.0065, and 2.038 derived by Che and Tench (4) for the chain radicals —CF_2—CF(OO)—CF_2— at 77 K.

Table 1. ^{17}O coupling constants for protein peroxides, X—$O^{(1)}$—$O^{(2)}$

Parent protein	Coupling atom	Component separations $\Delta H_\parallel$(G)	Effective couplings,* MHz A_f‡	B	Spin densities† ρ_{2s}	ρ_{2p}
Zein	$^{17}O^{(1)}$	46 ± 2	(−)45	(−)42	0.010	0.29
	$^{17}O^{(2)}$	68 ± 2	(−)62	(−)65	0.013	0.45
Edestin	$^{17}O^{(1)}$	42 ± 2	(−)45	(−)37	0.010	0.26
	$^{17}O^{(2)}$	71 ± 2	(−)62	(−)69	0.013	0.48

* Signs are not measured but are theoretically negative.
† Calculated with atomic coupling values $A_{2s} = -4628$ MHz and $B_{2p} = -144$ MHz (ref. 8, pp. 337, 338).
‡ Values assumed from measurements of liquids (see text).

CONCLUSIONS

The combined spin densities on $O^{(1)}$ and $O^{(2)}$ derived for edestin and for zein, 0.74, are not unity, as would be expected for an unpaired electron entirely in a π orbital on the two oxygens for which orbital-overlap distortions are neglected. This discrepancy might be interpreted to indicate some spreading of the π orbital of the unpaired electron to the carbon or to another atom of the protein. Also, some reduction in the effective B values and derived p_π spin densities is expected to result from rather large torsional oscillations of the peroxide group about the C—O bond. Such oscillations would reduce the observed maximum coupling below that expected for a static, parallel alignment of the p orbital as was assumed in the derivations. If the entire reduction is attributed to these oscillations and the $2p_\pi$ spin

Table 2. Approximate g values of protein-peroxide radicals

Parent protein	g_u	g_v	g_w
Zein	2.001	2.007	2.044
Edestin	2.002	2.006	2.040

density on the two oxygens is normalized to unity, the indicated $2p_\pi$ spin densities are 0.39 and 0.61 for $O^{(1)}$ and $O^{(2)}$ of zein peroxide and 0.35 and 0.65 for $O^{(1)}$ and $O^{(2)}$ of edestin peroxide. The small $2s$ spin densities are attributed entirely to spin-polarization effects and do not influence the calculations of ρ_{2p}.

These measurements of ^{17}O hyperfine structure verify that the ESR signals produced by exposure of these irradiated proteins to molecular oxygen are due to peroxide radicals, as earlier postulated.

This work was supported by Grant DAAG 29-77-G-0007 from the Army Research Office.

1. Gordy, W., Ard, W. B. & Shields, H. (1955) *Proc. Natl. Acad. Sci. USA* **41,** 983–996.
2. Patten, R. A. & Gordy, W. (1964) *Radiat. Res.* **22,** 29–44.
3. Rexroad, H. N. & Gordy, W. (1959) *Proc. Natl. Acad. Sci. USA* **45,** 256–269.
4. Che, M. & Tench, A. J. (1976) *J. Chem. Phys.* **64,** 2370–2374.
5. Melamud, E., Schlick, S. & Silver, B. L. (1974) *J. Magn. Reson.* **14,** 104–111.
6. Fessenden, R. W. & Schuler, R. H. (1966) *J. Chem. Phys.* **44,** 434–437.
7. Adamic, K., Ingold, K. U. & Morton, J. R. (1970) *J. Am. Chem. Soc.* **92,** 922–923.
8. Gordy, W. (1979) *Theory and Applications of Electron Spin Resonance* (Wiley-Interscience, New York).